

SOLAR PARTICLE EVENTS WITH HELIUM-OVER-HYDROGEN ENHANCEMENT IN THE ENERGY RANGE UP TO 100 MeV nucl^{-1}

J. TORSTI¹, L. KOCHAROV¹, J. LAIVOLA¹, S. POHJOLAINEN², S. P. PLUNKETT³,
B. J. THOMPSON⁴, M. L. KAISER⁴ and M. J. REINER⁵

¹*Space Research Laboratory, Department of Physics, University of Turku,
FIN-20014 Turku, Finland*

²*Tuorla Observatory, University of Turku, FIN-21500 Piikkiö, Finland*

³*Universities Space Research Association, Naval Research Laboratory,
Washington, DC 20375, U.S.A.*

⁴*NASA Goddard Space Flight Center, Greenbelt, MD 20771, U.S.A.*

⁵*Raytheon ITSS, 4400 Forbes Blvd., Lanham, MD 20706, U.S.A.*

(Received 12 June 2001; accepted 12 July 2001)

Abstract. Flux measurements of solar energetic particles (SEPs) in the ERNE instrument onboard SOHO indicate that the abundance of ^4He -nuclei compared to protons in the energy range up to 100 MeV nucl^{-1} was exceptionally high during the particle events on 27 May 1998 and 28 December 1999. The $^4\text{He}/\text{p}$ ratio stayed between 0.15–0.50 for more than ten hours. There was also a prolonged enhancement in helium-3, $^3\text{He}/^4\text{H} \approx 1\%$. Observations of EIT and LASCO on board SOHO confirm that the originators of both SEP events were western eruptions, flares and coronal mass ejections (CMEs). The onset of the SEP release took place close to the maximum of flares which were probably triggered by the rising CMEs. The observations suggest that the SEP events were started with the flare-(pre)accelerated particles, but impact of the CME-associated shocks might explain the continuation and modification of the helium and proton fluxes well after the flare production. These observations support the idea that the helium enhancements in the CME-associated events reflect the availability of seed particles that originate previously in flares.

1. Introduction

The abundance and isotopic composition of helium in the Sun is critical for many facets of solar physics (Laming and Feldman, 1994; Hansteen, Leer, and Holzer, 1997; Share and Murphy, 1998, and references therein). Early studies of the relative abundance of helium to proton in solar energetic particles (SEPs) were summarized by Van Hollebeke (1975) and Ramaty *et al.* (1978). In particular it was found that small events have an abundance of ^4He of 5–30% relative to protons, whereas in large events the helium-to-proton ratio is typically $\approx 1\%$ (e.g., Figure 7 in the review by Kocharov and Kocharov, 1984). The difference in the $^4\text{He}/\text{p}$ abundance observed in SEPs at 6–20 MeV/ nucl^{-1} was named among the distinctive properties of the impulsive vs. gradual SEP events (Kocharov, Kovaltsov, and Kocharov, 1983; Reames, Cane, and von Rosenvinge, 1990; Cliver, 1996). The ion acceleration in impulsive events with high $^4\text{He}/\text{p}$ is presently ascribed to flares, but in gradual



events with low ${}^4\text{He}/\text{p}$ to CMEs (Reames, 1999). To the best of our knowledge, the high values of helium-to-proton ratio, $>10\%$, being observed at energies well above $20 \text{ MeV}/\text{nucl}^{-1}$ in association with CMEs, have never been reported.

Using spectroscopic measurements by the SUMER instrument on the Solar and Heliospheric Observatory (SOHO) the photospheric abundance of helium was determined as $8.5 \pm 1.3\%$ (Feldman, 1998) and the coronal abundance as $5.2 \pm 0.5\%$ (Laming and Feldman, 2001). Solar atmospheric and accelerated helium abundances at the flare site can be determined with methods of γ -ray spectroscopy (Kozlovsky and Ramaty, 1974; Mandzhavidze, Ramaty, and Kozlovsky, 1997, 1999; Share and Murphy, 1997, 1998; Murphy *et al.*, 1997). These studies suggest either accelerated ${}^4\text{He}/\text{proton}$ ratios $\gtrsim 50\%$ and/or a higher He/H abundance in the sub-coronal regions than in the photosphere. In contrast, long-term measurements of the solar wind typically give smaller He/H ratios. The average ratios in the slow solar wind and in the high-speed streams are 3.5% and 5% , respectively; however, the ratio can be highly variable on short time scales, ranging from 0.1% to over 30% (Neugebauer, 1981; Gloeckler and Geiss, 1989; Bochsler, 1998; Geiss, 1998).

Not only the abundance ratio of energetic helium to proton but also the development of the ratio may be important. The falling ratio is what one may expect either due to overlapping of the flare accelerated and the CME accelerated particles or due to the rigidity-dependent interplanetary transport through the pre-existing (external) waves in the interplanetary medium. Reames, Ng, and Tylka (2000) reported that there have been observations of both falling and rising ${}^4\text{He}/\text{p}$ time profiles in the beginning of energetic particle events. According to the model by Ng, Reames, and Tylka (1999) the initial behavior of the ratio is a matter of the size of the SEP event. The rising ${}^4\text{He}/\text{p}$ profiles were explained by the ion propagation through the proton-amplified (self-generated) waves expected to dominate in strong events. The model was applied to a gradual event with $\text{He}/\text{p} \approx 1\%$ in the $11\text{--}22 \text{ MeV nucl}^{-1}$ energy range (Reames, Ng, and Tylka, 2000).

In the present paper we report two atypical SEP events with ${}^4\text{He}/\text{p} > 10\%$ persisting during many hours in the energy range up to $100 \text{ MeV nucl}^{-1}$. We use the helium and proton observations of the Energetic and Relativistic Nuclei and Electron experiment (ERNE) (Torsti *et al.*, 1995) on board SOHO. ERNE consists of low- and high-energy particle telescopes, LED and HED. In the case of protons and helium the detected energy ranges are $1.6\text{--}13 \text{ MeV nucl}^{-1}$ and $12.5\text{--}100 \text{ MeV nucl}^{-1}$ for LED and HED, respectively. The two events under investigation started on 27 May 1998 and 28 December 1999. Due to repetitive occurrences of solar particle eruptions before those dates and, as a consequence, enhanced background fluxes, especially at low energies, we focus on the energy range $> 12.5 \text{ MeV nucl}^{-1}$, i.e., on the HED observations. The large view cone of HED with geometric factor $26\text{--}36 \text{ cm}^2 \text{ sr}$, depending on energy, offers sufficient statistics on the development of protons and helium fluxes during both events. It is also important that HED allows high-precision anisotropy measurements, which are necessary for estimates of the interplanetary transport conditions. The aim of

this work is to analyze the ion time profiles and to identify the processes that might have been responsible for the development of the helium and proton fluxes. For this purpose we employ solar images from SOHO and *Yohkoh*, the radio data recorded onboard WIND, and optical and radio data from the ground-based observatories.

2. Observations

2.1. EVENT SELECTION

We have undertaken a search for relatively large SEP events enhanced in helium. The survey covered all events collected by ERNE during the SOHO flight from the launch in December 1995 until March 2000. The survey did not include, due to the non-operational status of the spacecraft, the periods from 25 June until 9 October 1998, and from 21 December 1998 until 8 February 1999. In addition, there are other time intervals of a few days when ERNE was not in an operation mode. The criteria of the survey were: (a) the helium intensity at maximum is greater than 10 fold compared to the galactic background in energy channel 13–26 MeV nucl^{-1} ; (b) intensity enhancement above the background is significant in energy range 26–51 MeV nucl^{-1} ; and (c) the ${}^4\text{He}$ -to-proton intensity ratio is more than 10% in energy range > 13 MeV nucl^{-1} . As a result of the survey we found only two events fulfilling the criteria, the events on 27 May 1998 and 28 December 1999. This is not very surprising, because the helium-rich events are typically small.

The intensity-time profiles of protons and ${}^4\text{He}$ during the event periods in May 1998 and December 1999 are shown in Figure 1. On 27 May 1998, the first arrival of particles in the energy channel 25–50 MeV nucl^{-1} was registered at about 14:10 UT. The major helium-rich event continued until about 04 UT next day, when a new rise of the proton intensity started and the ${}^4\text{He}/p$ ratio dropped by one order of magnitude. Hence, we limit our analysis to the period from 14 UT 27 May to 04 UT 28 May 1998. In the December event, the first particles in the energy range 26–51 MeV nucl^{-1} were registered at about 02:20 UT. One can see from Figure 1 that there were no significant new particle enhancements during 40 hours from the start. The time intervals selected for the analysis of both events are shown in Figure 1 with vertical lines. In the following we call the 27 May 1998 and 28 December 1999 events, respectively, as events A and B.

2.2. SEP INTENSITY-TIME PROFILES

The intensity-time profiles of protons and helium during events A and B are plotted in Figure 2. Both the intensity and the time are presented in logarithmic scale. To make comparisons with electromagnetic solar observations in the beginning of the event easier we use a shifted time,

$$t_{\text{shift}} = t_{\text{obs}} - \frac{s}{v} + \frac{1 \text{ AU}}{c}, \quad (1)$$

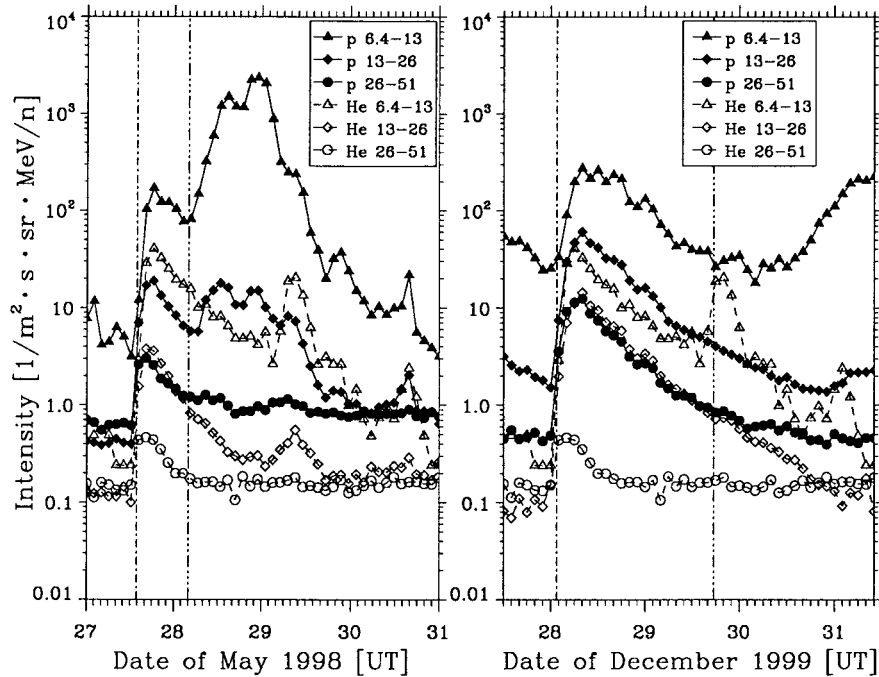


Figure 1. Two-hour average intensities of protons and ^4He in three energy channels during the SEP events 27 May 1998 (left) and 28 December 1999 (right). The energy channels in MeV nucleon^{-1} are shown in the legend for both ^4He (open symbols) and protons (closed symbols). The pair of vertical lines bracket selected periods of the high $^4\text{He}/\text{p}$ ratio in the energy range above $13 \text{ MeV nucleon}^{-1}$.

where t_{obs} is the time of the particle registration at SOHO, v is the particle speed, c is speed of light, and s is the mean length of the particle flight trajectory guided by the interplanetary magnetic-field line connecting Sun to SOHO. The solar wind measurements with the proton monitor of the Charge, Element and Isotope Analysis System (CELIAS) (Hovestadt *et al.*, 1995) on board SOHO indicate that the solar wind speed was about 365 km s^{-1} and 474 km s^{-1} during the arrival of first particles of events A and B, respectively. As the path length we use the length of the Archimedean spiral line multiplied by the additional form-factor of 1.1 accounting for the pitch-angle distribution of first arriving particles, i.e., we adopt the length value $s = 1.32 \text{ AU}$ and $s = 1.25 \text{ AU}$ respectively for A and B. Note that the form-factor should rise in the course of event as more scattered particles arrive at SOHO. This is not included in the s value employed in Equation (1), but the resulting inaccuracy is masked to some extent by applying the logarithmic scale to time. A transformation of the Equation (1) type cannot account for the variance of the particle trajectories, which may be significant if the interplanetary transport is not scatter-free. Nevertheless a presentation of SEP data in the form of the shifted-time profiles is still helpful for a study of the first particle injection and also for the preliminary analysis of the late development. However, a final interpretation of the

particle flux profiles cannot be justified without SEP anisotropy data, which must be and will also be employed.

Based on observations in the HED channels (Figure 2, $E > 12.5 \text{ MeV nucl}^{-1}$), we conclude that in event A the solar release of both protons and ^4He took place at $t_{\text{shift}} = 13:30 \text{ UT} (\pm 5 \text{ min})$. Limited statistics and the extension of the fluxes from the previous event in energy channels below 10 MeV does not allow us to make any strict conclusions on the onset in low-energy channels. However, it seems possible that the release took place at the same time as in the high-energy channels. In the energy range 12.5–25 MeV nucl^{-1} the intensity achieved the maximum, 20 protons $\text{m}^{-2} \text{ s}^{-1} \text{ sr}^{-1} (\text{MeV nucl}^{-1})^{-1}$ and 4 ^4He -ions $\text{m}^{-2} \text{ s}^{-1} \text{ sr}^{-1} (\text{MeV nucl}^{-1})^{-1}$, respectively in 3.6 and 2.3 hours time. The intensity change from background to maximum was, respectively, 50 and 40 fold.

Using the high-energy observations during the event B (Figure 2) we conclude that the first energetic helium release took place at $t_{\text{shift}} = 01:20 \text{ UT} (\pm 8 \text{ min})$. Injection of the first protons above the background level occurred at $t_{\text{shift}} = 01:50 \text{ UT} (\pm 5 \text{ min})$. The rise to the maximum in the energy range 12.5–25 MeV nucl^{-1} takes about 7.3 and 5.2 hours for protons and ^4He , respectively. The intensity maxima are 50 $\text{p m}^{-2} \text{ s}^{-1} \text{ sr}^{-1} (\text{MeV nucl}^{-1})^{-1}$ and 10 $^4\text{He m}^{-2} \text{ s}^{-1} \text{ sr}^{-1} (\text{MeV nucl}^{-1})^{-1}$. Thus the maximum intensities of protons and ^4He during the event B are 2.5-fold higher than during A. In proton channels 2.7–5.1 and 5.1–10 MeV, and He-channel 2.7–5.1 MeV nucl^{-1} , the start of the intensity rise is delayed until to $\approx 03 \text{ UT}$. The enhanced background levels due to the previous event may mask the start in the low-energy channels, where the rise seems gently inclined and weak.

With HED data, the proton anisotropy can also be deduced and the interplanetary mean free path can be ascertained. The parallel mean free path of 12.5–25 MeV protons near the Earth, $\Lambda_{\parallel}(r = 1 \text{ AU})$, is estimated to be about 0.35 AU for both events A and B. To obtain this estimate we employed a model of focused transport with isotropic scattering at a constant radial mean free path throughout the interplanetary medium¹ and compared the time-integrated (steady-state) theoretical anisotropy with a steady-state value of anisotropy observed with HED during 2–9 hours after the event onset. The moderate value of the mean free path suggests that the interplanetary medium was not very turbulent, and seeing conditions in SEPs correspondingly were not very poor, so that one might expect that the shifted-time technique (Equation (1)) allows a reasonable estimate for the qualitative description of the SEP production scenario. Note that for the scenario estimate, one should keep in mind that under these transport conditions even impulsive solar injections would result in a significantly long increase in the near-Earth intensity, which however would be still much shorter than the increase actually observed (cf., theoretical curves and experimental profiles in Figure 2).

¹The employed transport code is similar to the IAS code by Kocharov *et al.* (1998) with rigidity-independent mean free path.

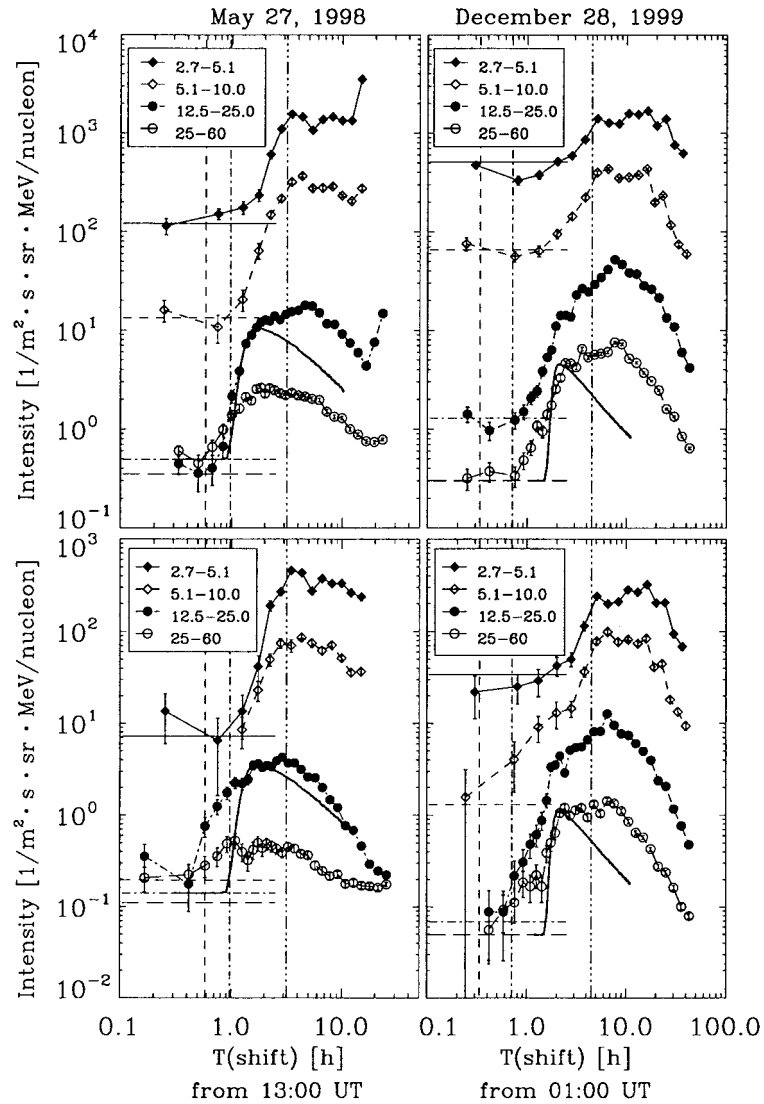


Figure 2. Intensity profiles of protons (*upper row*) and α -particles (*lower row*) as a function of shifted time. The *points* represent the ERNE observations in four energy channels during the events (A) 27 May 1998 (*left*) and (B) 28 December 1999 (*right*). The background intensities during three hours preceding the event start are given with the same *horizontal lines* as the lines connecting the points. The *vertical dashed lines* show the maximum time of the corresponding soft X-ray flare. *Vertical dash-dot* and *dash-dot-dot* lines indicate instants of time when the CME leading-edge arrived at heliocentric distances $5 R_{\odot}$ and $15 R_{\odot}$, respectively. *Solid curves* additionally illustrate 12.5–25 MeV nucl^{-1} and 25–60 MeV nucl^{-1} profiles that might be expected in the case of impulsive injection of SEPs at the instant of shifted time $t_{\text{inj}} = 14:05$ UT and $02:40$ UT, respectively for the events A and B.

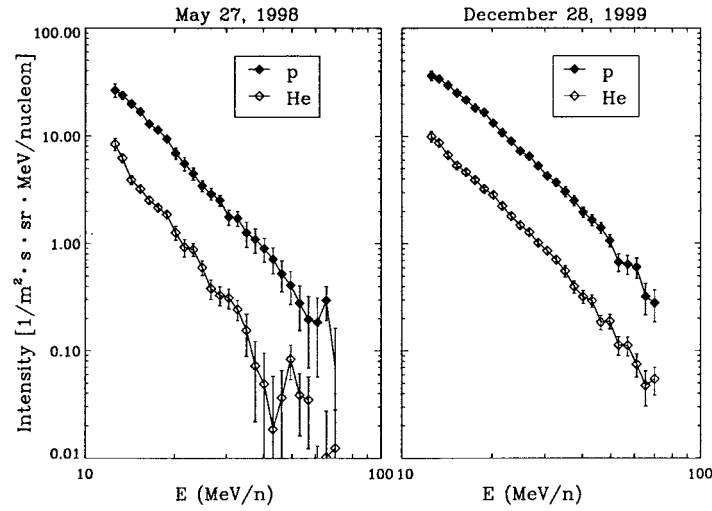


Figure 3. Average energy spectra of protons and ^4He during the periods (A) 14 UT 27 May – 04 UT 28 May 1998, and (B) 02 UT December 28 – 18 UT 29 December 1999.

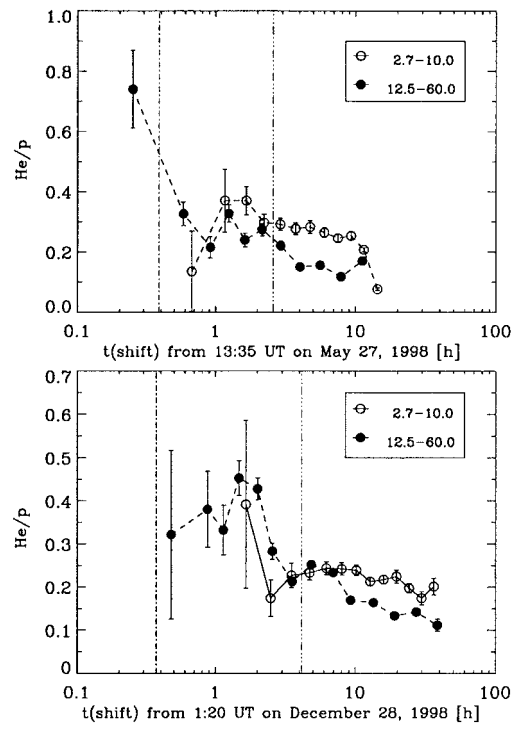


Figure 4. The abundance ratios of ^4He to proton fluxes during the events A (upper panel) and B (lower panel) vs. shifted time in two energy ranges, 2.7–10 MeV nucleon^{-1} and 12.5–60 MeV nucleon^{-1} . Vertical lines show the location of the CME leading edge at $5 R_{\odot}$ and $15 R_{\odot}$.

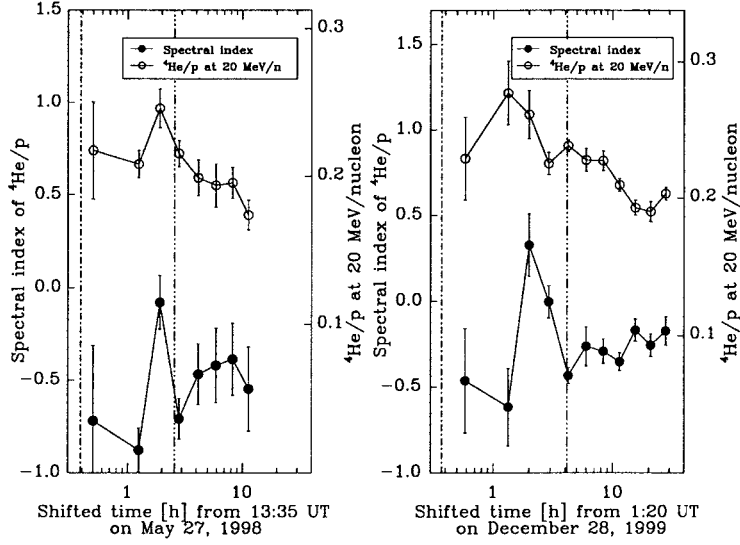


Figure 5. Development of the ${}^4\text{He}/\text{p}$ spectral index, η , for the energy range 12.5–60 MeV nucl^{-1} during events A (left panel) and B (right panel). Corresponding values of the coefficient $({}^4\text{He}/\text{p})_{20 \text{ MeV } \text{nucl}^{-1}}$ in Equation (2) are shown with open symbols. Vertical lines show the location of the CME leading edge at $5 R_{\odot}$ and $15 R_{\odot}$.

2.3. HELIUM ABUNDANCE

Time-integrated energy spectra of protons and helium-4 are shown in Figure 3. The figure reveals the distinctive property of these two events: the helium enhancement persists through the high energies, above 70 MeV nucl^{-1} . The energy spectra are close to the common flare particle spectrum $\sim E^{-3}$.

Time profiles of the ${}^4\text{He}/\text{p}$ ratio in two energy channels, 2.7–10 and 12.5–60 MeV nucl^{-1} , are shown in Figure 4. The ratio stays at a very high level, around $\approx 20\text{--}30\%$, most of the time in both events A and B (27 May 1998 and 28 December 1999). The ${}^4\text{He}/\text{p}$ ratio behaves smoothly during the period 2.5–10 hours from the onset in both energy ranges. The lower-energy ${}^4\text{He}/\text{p}$ -ratio exceeds the higher-energy ratio by about 50% in the event A and less essentially in the event B. There was a very strong He enhancement in the beginning of the event A, whereas during the first hour of event B the statistics were not high enough for significant conclusions on the development of ${}^4\text{He}/\text{p}$. However, in the subsequent phase of event B a gradual decrease of the high-energy ${}^4\text{He}/\text{p}$ ratio seems possible.

A change in the acceleration mechanism could leave its imprints also in the ion spectrum evolution. We have plotted, however, not the spectra of protons and helium but the energy dependence of their ratio, because the intensity ratio is expected to be immune to the intensity fluctuations. The deduced energy dependence of the ${}^4\text{He}/\text{p}$ ratio was found to be close to a power law in energy. The corresponding power-law spectral index is shown in Figure 5. Thus Figure 5 plots the spectral

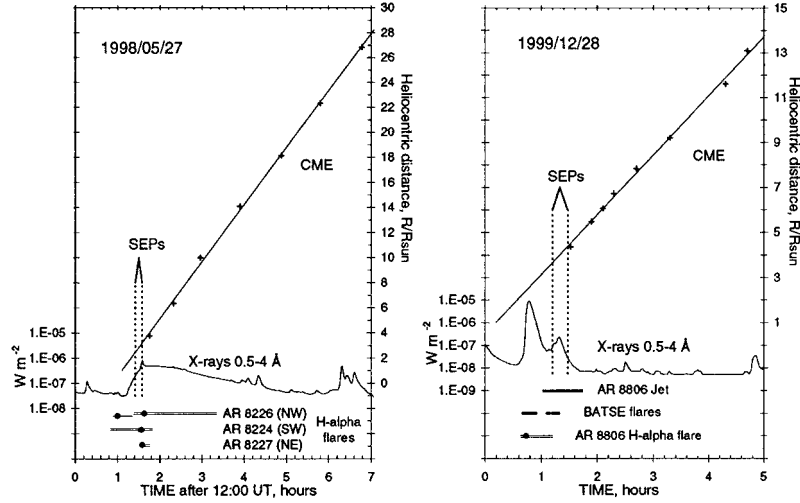


Figure 6. LASCO/SOHO CME height–time data (R/R_{\odot}) and *GOES 9* soft X-ray flux at 0.5–4 Å (W m^{-2}) for the events A (left panel) and B (right panel). The durations (maxima) of the H α flares are marked with horizontal bars (points). First energetic He injection time is shown with the vertical pair lines labeled SEPs. Note that the SEP injection continues for many hours next to the first injection time marked in the figure.

index, η , of the best power-law fit to the observed energy dependence of the ${}^4\text{He}/\text{p}$ ratio in the energy-range 12.5–60 MeV nucl^{-1} ,

$${}^4\text{He}/\text{p} = \left(\frac{{}^4\text{He}}{\text{p}} \right)_{20 \text{ MeV } \text{nucl}^{-1}} \left(\frac{E}{20 \text{ MeV } \text{nucl}^{-1}} \right)^{\eta}, \quad (2)$$

in a particular interval of the shifted time. We also show the estimated ${}^4\text{He}/\text{p}$ ratio at 20 MeV nucl^{-1} corresponding to the best power-law fit. The ${}^4\text{He}/\text{p}$ spectral-index seems peaked at around 2 h (relative time), followed by a steady-state period after 4 h (Figure 5). Note that in event B the transition to the steady-state phase occurs simultaneously with bending of the 5.1–25 MeV nucl^{-1} ${}^4\text{He}$ intensity-time profiles seen in Figure 2 at around 3 hr.

In both events A and B, the ERNE instrument also detected a moderate enhancement of the ${}^3\text{He}$ flux in the energy range > 10 MeV nucl^{-1} . However, a poor count statistics does not allow a study of differential distributions of the isotopic abundances. The time-integrated ${}^3\text{He}/{}^4\text{He}$ ratio was in the range 0.5–2.5% during both events.

2.4. SOLAR OBSERVATIONS

We summarize observations of solar electromagnetic emissions relevant to the energetic particle events A and B. Both events were associated with LASCO CMEs. In both events the CME first-appearance time preceded the corresponding injection time of first protons and helium. We consider a time period starting around the

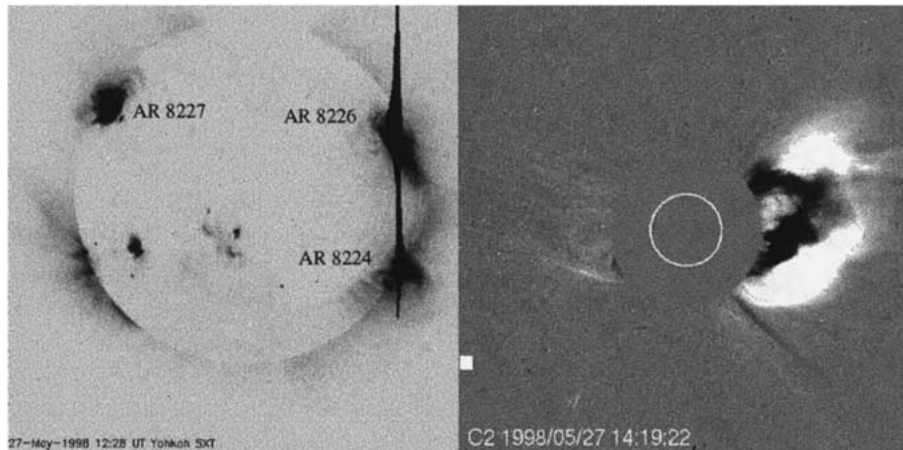


Figure 7. SXT/Yohkoh full-disk image on 27 May 1998 at 12:28 UT (*left*) and difference image of the LASCO/SOHO CME at 14:19 UT (*right*). The three active regions (AR 8226, AR 8224, and AR 8227) that produced H α flares during the period under analysis are marked on the image. Note the large trans-equatorial soft X-ray loop connecting AR 8226 and AR 8224 just below the LASCO CME.

extrapolated CME lift-off time and extending beyond the first SEP injection time (Figure 6).

2.4.1. The 27 May 1998 Event

Solar Geophysical Data (SGD, 1998) list a variety of solar processes in the vicinity of the first particle injection time or the event A, 13:30 UT (± 5 min) on 27 May 1999. H α flares were observed in three different regions: in NOAA AR 8226 (N18 W60) the H α flare peaked at 13:00 UT and at 13:28/13:38 UT, in AR 8224 (S12 W80) at 13:33 UT, and in AR 8227 (N22 E51) at 13:35 UT. The GOES soft X-ray flux started to rise around 13:15 UT, and at 13:35 UT a flux peak of GOES class C7.5 was observed. Timing of the H α flares and the GOES soft X-ray profile are shown in Figure 6. A full-disk Yohkoh/SXT (Tsuneta *et al.*, 1991) pre-flare image at 12:28 UT is presented in Figure 7, together with the active region locations. During the estimated first particle release time Yohkoh SXT was observing the region around AR 8226 in flare mode, and saw plasma flows along the large loop structures.

Figure 7 also shows a coronal mass ejection observed with LASCO onboard SOHO (Brueckner *et al.*, 1995). The CME was seen in the LASCO/C2 images starting with the frame at 13:13 UT. Analysis of the CME height–time data has revealed a constant speed profile of 880 km s $^{-1}$ (the leading edge speed at the position angle 304 $^{\circ}$). A linear extrapolation of the leading-edge distances back to the solar surface yields the nominal lift-off time \approx 13:05 UT. There were a number of events in electromagnetic emissions observed during the pre-event period, 13:00–13:30 UT, a period from around the nominal CME lift-off to the time of the first

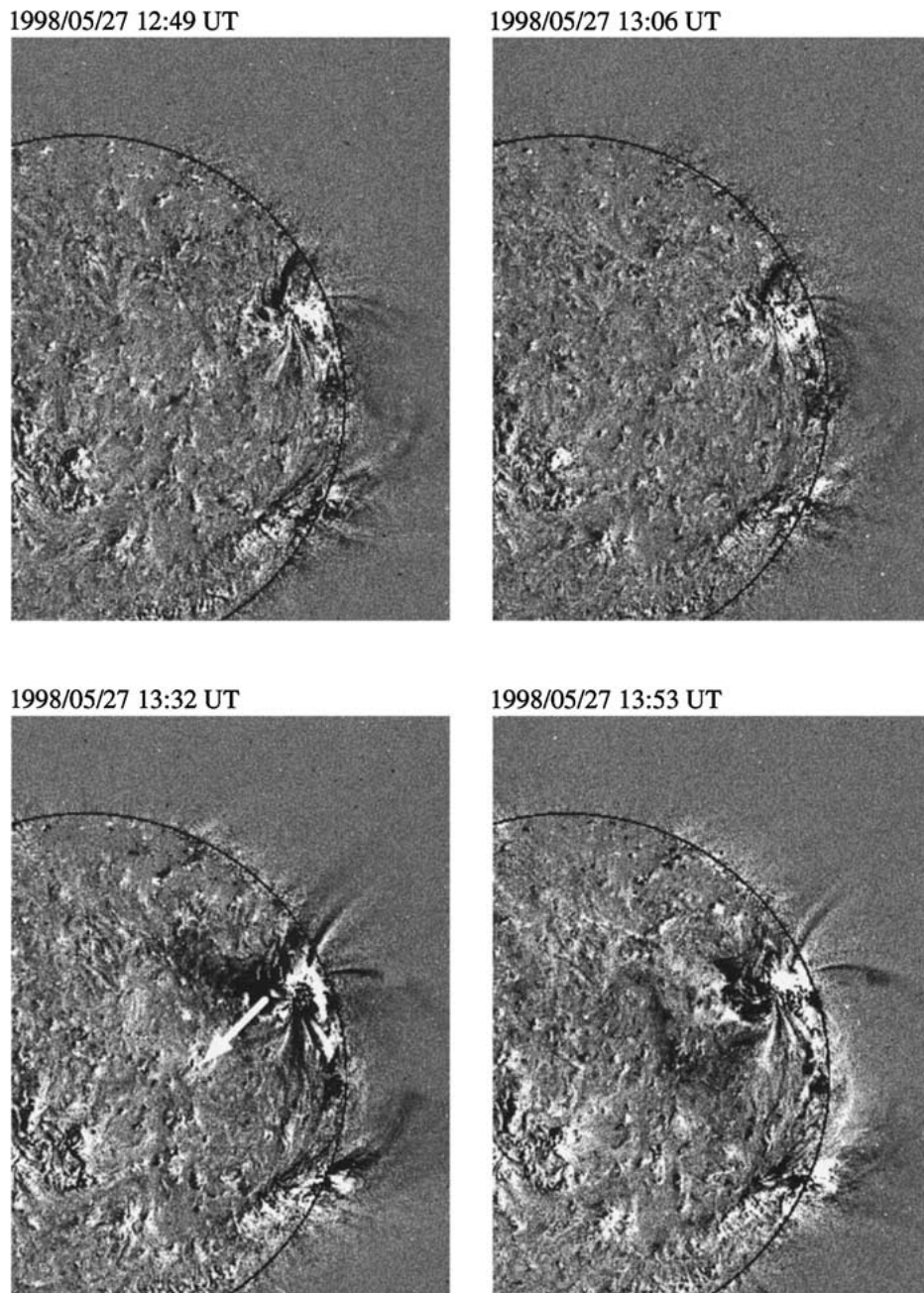


Figure 8. EIT/SOHO successive difference images in the Fe line 195 Å on 27 May 1998. The time moments 12:49, 13:06, 13:32, and 13:53 UT show the latter times of each pair of images. The *arrow* indicates propagation of a Moreton wave from the NW.

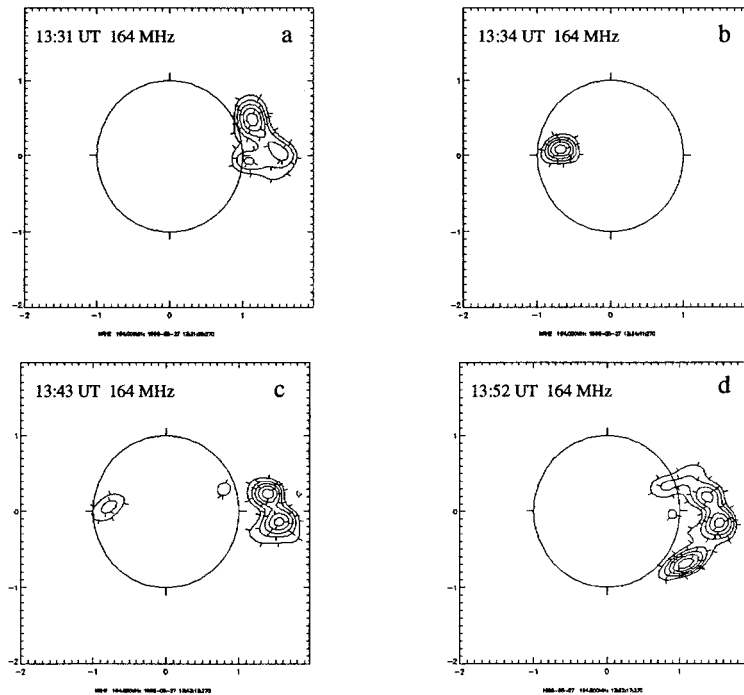


Figure 9. Nançay radioheliograph full-disk images of the Sun at 164 MHz on 27 May 1998. The long-duration radio type IV emission during 13:06–13:32 UT was located over the large-scale loop structure near AR 8226, an example is shown in (a). Radio type III bursts occurred near the active region in the northeast during 13:32–13:36 UT, burst location is shown in (b). These type III bursts were strong enough to over-shadow the emission coming from the western loop system. During 13:42–13:54 UT several type III burst groups occurred at different locations, examples in (c) and (d).

energetic particle injection. There was a metric type III burst at 13:02 UT. Optical observations registered a subflare in AR 8226 (N19 W66) with maximum at 13:00 UT. The SOHO EUV Imaging Telescope (EIT) (Delaboudinière *et al.*, 1995) also observed a flare eruption in this active region near the west limb. The EIT 195 Å running difference images show brightenings propagating away from AR 8226, starting from 13:06 UT (Figure 8). A bright front is seen in the 13:32 UT difference image, heading southeast (marked by arrow in Figure 8), followed by a dark front in the difference image at 13:53 UT. These indicate a coronal Moreton wave (EIT wave) propagating away from AR 8226 concurrently with the CME lift-off. Note also a dimming in this event, seen in the 13:32 and 13:53 original (not difference) images, a dark area directly to the east of the flaring region. The dimming was observed close to the first SEP injection time. Additionally, there may be a small area of dimming north of the active region in the south.

The Tremsdorf radio spectrometer (Mann *et al.*, 1992) recorded dynamic spectra in the 40–800 MHz frequency range, and the Nançay radioheliograph (Kerdraon and Delouis, 1997) imaged the same time period at five separate frequencies.

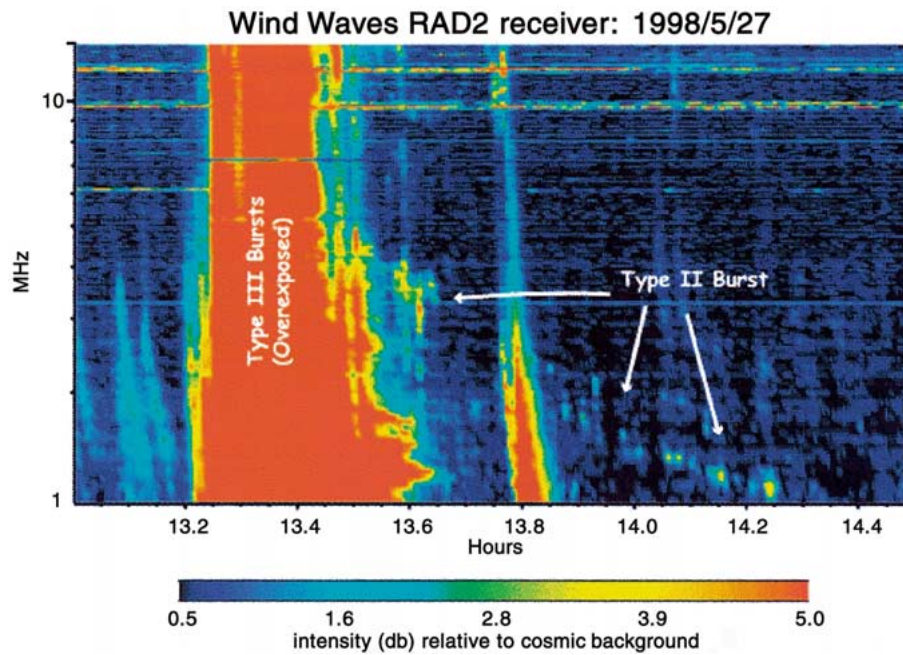


Figure 10. Dynamic spectrogram of interplanetary radio emissions registered by the WAVES experiment onboard WIND. The emissions comprise type III bursts and a weak intermittent type II (chain of yellow-to-blue points between 13:30–14:20 UT).

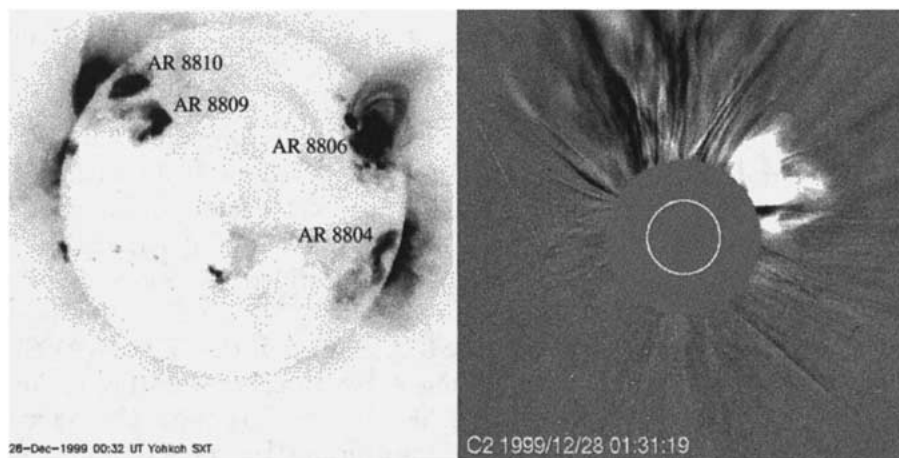


Figure 11. SXT/Yohkoh full-disk image on 28 December 1999 at 00:32 UT (left) and difference image of the LASCO/SOHO CME at 01:31 UT (right). There are several active regions on the disk, but only one of them is known to have flared in $H\alpha$ (AR 8806). Note also the large loops of an active region that has rotated behind the limb, in the southwest. There seems to be some evidence of interconnecting loops between this region and AR 8806.

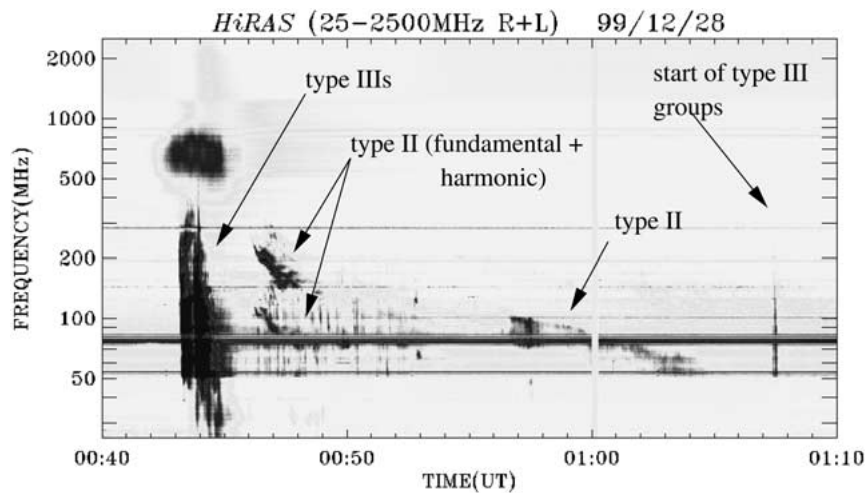


Figure 12. HiRAS dynamic spectra at decimetric–decametric waves on 28 December 1999, during 00:40–01:10 UT. The first GOES class M4.5 burst was associated with a group of type III bursts starting around 00:43 UT, followed by fluctuations and two separate radio type II bursts (marked by arrows). A second group of less intense radio type III bursts started around 01:07 UT, lasting up to 01:20 UT.

During 13:06–13:32 UT a radio type IV emission was observed in the spectra, which could be associated with emission coming from the large scale loop system over the solar northwestern limb (Figure 9(a)). Following this long-duration radio event several metric type III bursts were observed: at 13:32–13:36 UT located over the active region in the northeast (Figure 9(b)), coinciding with the start of the H α flare in AR 8227, and during the period 13:42–13:54 UT (Figures 9(c) and (d)) located over different regions on the disk.

No metric type II is reported in *SGD* (1998), but the WIND/WAVES experiment registered a weak intermittent type II burst during 13:30–14:20 UT in the frequency range 4000–1000 kHz (Figure 10), which might correspond to a shock traveling during that period from heliocentric distance $\approx 3.5 R_{\odot}$ to $10 R_{\odot}$. This emission is visible after the hectometric type III, which dominates during 13:15–13:25 UT with an upper frequency limit of about 60 MHz (the latter is evident from the Trensdorf spectrogram). Thus the first SEP injection coincides in radio emissions with the end of the type IV burst associated with a large loop system over the western limb, with the type III bursts injected from coronal altitudes $\approx 0.3 R_{\odot}$, and with the hectometric type II already at heliocentric distances $\approx 3.5 R_{\odot}$.

2.4.2. The 28 December 1999 Event

Event B was associated with a CME and two impulsive soft X-ray flares (see Figure 6). Fitting height–time data of the CME at phase angle 292° revealed a constant speed profile of 512 km s^{-1} and the extrapolated-to-surface start time 00:10 UT (the first appearance time in LASCOC2 is 00:54 UT). The GOES satellites observed

two soft X-ray bursts close in time, the first one starting at 00:39 UT (reaching GOES class M4.5) and the second one starting at 01:12 UT (reaching C2.8 at 01:20 UT). A class 2B H α -flare was reported to start in AR 8806 (N20 W56) at 00:42 UT (SGD, 2000), but it ended at 01:11 UT, just at the time the second GOES burst started. No EIT wave was observed during this event. The Compton GRO BATSE instrument (Schwartz *et al.*, 1993) recorded an intense hard X-ray flare during 00:41–00:54 UT, and a series of smaller flares between 01:07 and 01:18 UT. The durations of the H α flare and the BATSE hard X-ray flares are also marked in Figure 6. The estimated release time for the first energetic helium ions (01:20 UT \pm 8 min) suggests association with the later GOES burst. Unfortunately *Yohkoh*/SXT was in satellite night time during this event and therefore no soft X-ray images are available. A pre-flare full-disk *Yohkoh*/SXT image at 00:32 UT is presented in Figure 11, which also shows the active region locations, and also the LASCO CME above AR 8806.

Intense metric–decimetric radio emissions were associated with the first GOES event starting with a group of type III bursts at 00:43 UT. Also a type V burst was reported in the 25–75 MHz range (SGD, 2000). Two metric type II bursts followed during 00:46–01:05 UT in the frequency range from 250 to 50 MHz (Figure 12) indicating coronal shocks probably driven by X-ray ejecta from the flare region (e.g., Klein *et al.*, 1999). The group of type III bursts, starting around 01:07 UT, was most likely connected to the start of the second GOES event. The type III bursts continued up to 01:20 UT at which time a radio type IV burst at 30–80 MHz was observed to start (SGD, 2000), lasting to 02:03 UT. Concurrently with the metric type IV burst the SEP injection began to rise. Unfortunately interplanetary radio data for this period are not available because of a technological break in the WIND/WAVES observations.

The second soft X-ray flare (C2.8) peaked at 01:20 UT, close to the onset time of the energetic ion eruption. Before that, between 01:07 UT and 01:18 UT, BATSE registered several hard X-ray pulses. A prominent feature of this event is a jet-like eruption observed by EIT/SOHO between 01:08–01:43 UT and shortly before that by *Yohkoh* in the NW active region AR 8806 (Figures 13 and 14). The jet was seen moving along the high loop leg in the high loop plus low arcade configuration beneath the CME. The EIT difference image at 01:08 UT (Figure 14) shows the location of the erupted loop over AR 8806, in the northwest (visible as a darker area), and a jet (visible as a bright strip). In the difference image at 01:21 UT a new bright area is visible, probably connected with the second soft X-ray burst. The jet was also visible at 01:21 UT, 01:31 UT and 01:43 UT. The EIT-observed jet, the radio type III and type IV fit well the start of the SEP injection in this event, whereas timing of the metric type II bursts (Figure 12) is inconsistent with SEPs observed at SOHO.

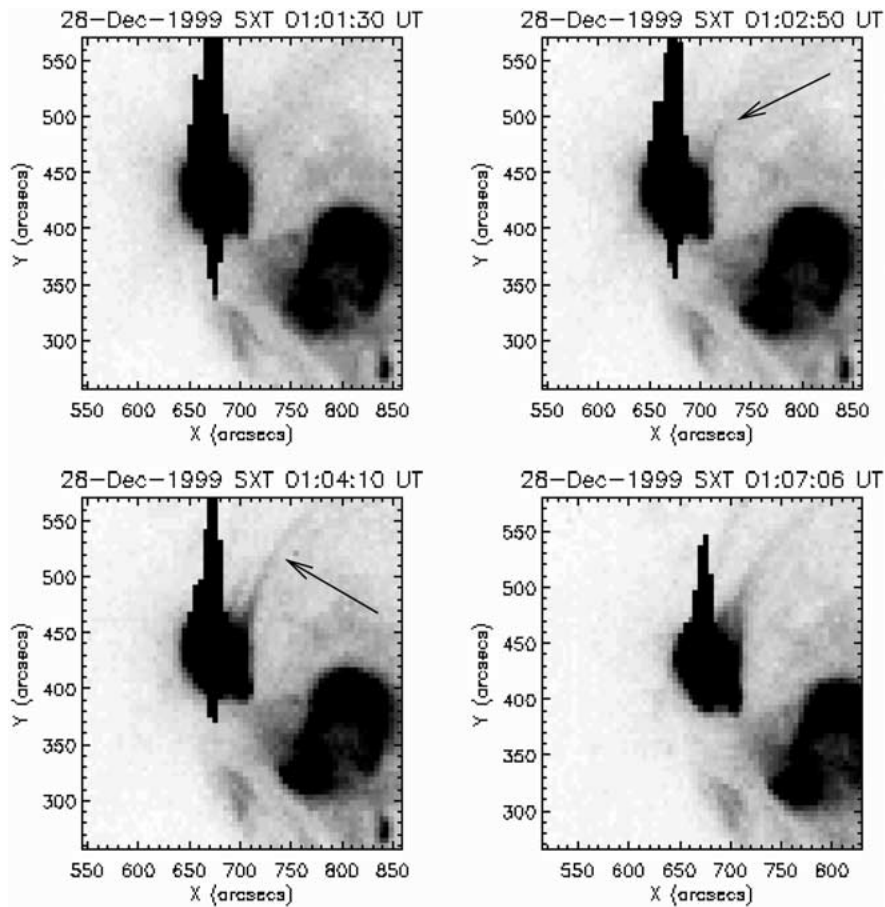


Figure 13. A jet-like eruption observed by SXT/Yohkoh on 28 December 1999, in AR 8806 (images are in negative; jet is shown with *arrow*). After 01:08 UT, a jet-like eruption was observed by EIT (see Figure 14).

3. Discussion

3.1. SOLAR ORIGINS OF THE HELIUM OVER PROTON ENHANCEMENT

The timing comparison between the observations of solar electromagnetic bursts and energetic particle injected towards the Earth shows that the initiator of particle acceleration process are in or in the vicinity of NOAA active regions 8226/8224 and 8806 during events A and B (Figures 6, 7, and 11). The angular distance on the solar surface between the location of the flare and the Earth-injection area was small, $\approx 10^\circ - 30^\circ$, during both A and B. Thus the flares were located well inside the region, which permits fast injection of flare accelerated particles to the root of the magnetic tube guiding particles to the Earth. However, a flare injection alone could not explain the observed duration of the events. This is evident from

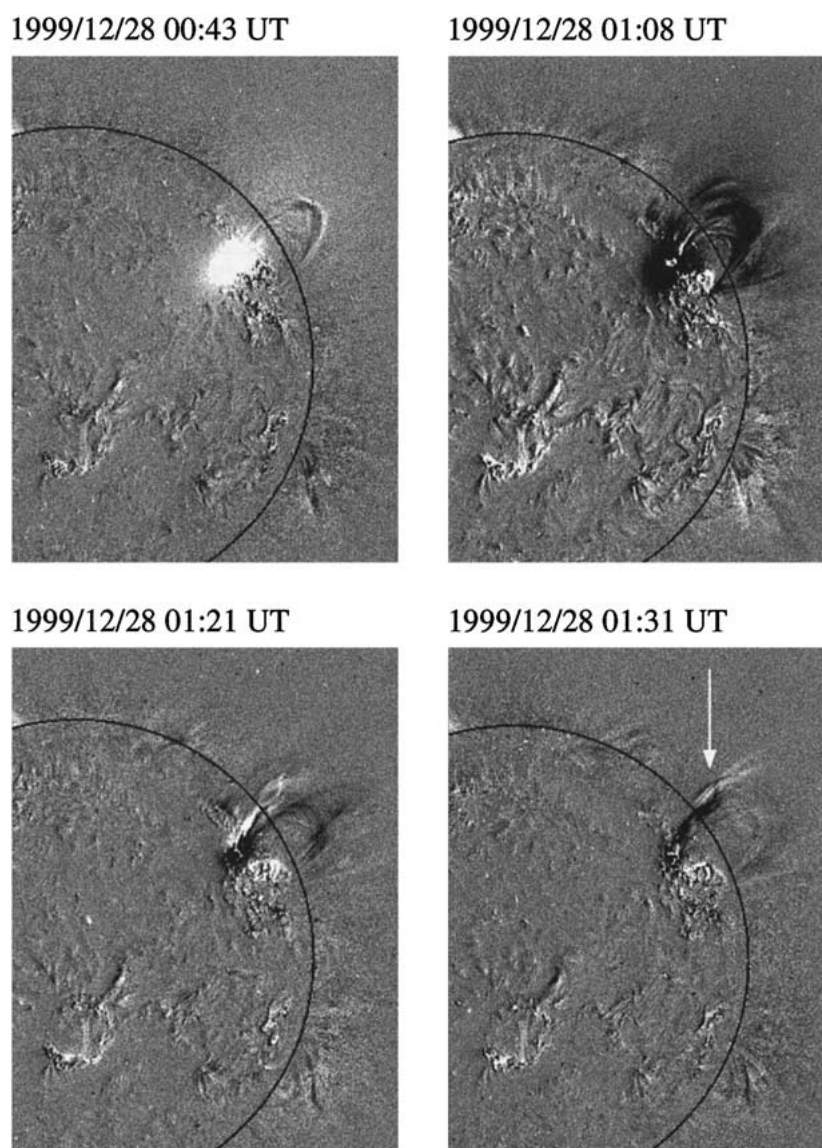


Figure 14. Difference images of the solar eruption observed by EIT in the Fe line 195 Å on 28 December 1999. The frame 00:43 UT shows the flare. A jet is seen in the successive difference images at 01:08, 01:21, and 01:31 UT (shown with *arrow*).

Figure 2, where we have compared the observed intensity-time profiles with profiles expected from an impulsive injection at the near-Earth parallel mean free path $\Lambda_{\parallel} = 0.35$ AU, corresponding to the observed anisotropy of the proton flux.

The exceptionally high ${}^4\text{He}/\text{p}$ ratio, and enhanced ${}^3\text{He}/{}^4\text{He}$ ratio leads us to conclude that the accelerated ions originated from the flaring plasma. A high ${}^4\text{He}/\text{p}$

ratio is not expected to have been created from the ambient solar wind by the interplanetary shock. According to SWEPAM/*ACE* observations (McComas *et al.*, 1998) the ${}^4\text{He}/\text{p}$ ratio in the solar wind stayed nominal during several days before and after both events. The solar wind value varied from $\approx 1\%$ to 4% , whereas in SEPs we observed the ${}^4\text{He}/\text{p}$ ratio up to $\approx 50\%$ (Figure 4). A flare is an obvious candidate for the initial acceleration phase. Mandzhavidze, Ramaty, and Kozlovsky (1999) determined the abundances of flare-accelerated helium isotopes based on γ -ray spectroscopy measurements of 20 flares. They found that there are flares that exhibit α -particle enhancements ($\alpha/\text{p} > 0.1$), and show evidence for presence of accelerated ${}^3\text{He}$. On the other hand, Reames (1994) determined the averaged ratio of elements from H to Fe in the energy range $1\text{--}4\text{ MeV nucl}^{-1}$ based on gradual SEP events analyzed by Breneman and Stone (1985) and Reames, Richardson, and Barbier (1991). According to this result the average abundance ratio of ${}^4\text{He}/\text{p}$ is $4.7 \pm 0.4\%$. The highest ${}^4\text{He}/\text{p}$ ratio among 43 gradual SEP events was 14% . The average ratio of events A and B in energy range $2.7\text{--}10\text{ MeV nucl}^{-1}$ is 27% and 20% , respectively, i.e. $4\text{--}6$ fold compared to the average in gradual events, and almost twice the highest among the 43 events.

As pointed out by Reames, Ng, and Tylka (2000), time differences might occur between energetic particle flux enhancement of various particle species close to Earth even though the particle release at the Sun started simultaneously and particles had the same velocity. If particles do have different rigidity they resonate during their interplanetary transport with different waves in the background wave spectrum. For strong events, also scattering by self-amplified waves might be important. Reames *et al.* compared He/p profiles for a small event and a large event, respectively on 8 May and 30 September 1998. Both were gradual events with maximum proton intensities of the order of $100\text{ protons}/(\text{cm}^2\text{ s sr MeV})$ and $3000\text{ protons}/(\text{cm}^2\text{ s sr MeV})$ in the energy range $2.1\text{--}2.5\text{ MeV}$. During the present events, A and B, the maximum proton intensities in energy range $1.8\text{--}3.3\text{ MeV}$ were of the order of $0.3\text{ protons}/(\text{cm}^2\text{ s sr MeV})$, which is well below the small event in the Reames *et al.* analysis. During the $> 2\text{ h}$ periods of the present events a change in the He/p ratio is either absent or weak (Figure 4). However, the descending He/p ratio during the first hour of event A may be produced by the ion transport through the background (not self-amplified) waves.

Meyer (1985) studied solar particle abundances and found that ${}^4\text{He}$ is particularly problematic because it does not behave like C as it should if both are fully stripped. Cane, Reames, and von Rosenvinge (1991) also found the behavior of ${}^4\text{He}$ is extraordinary. They attributed the high ${}^4\text{He}/\text{C}$ values to the presence of flare-heated material in some events. Based on the above arguments we conclude that energetic particle populations in A and B originate from the flare material, while the prolonged streaming of SEPs indicates that the ion acceleration extends well beyond the flare pulse. A peak of the ${}^4\text{He}/\text{p}$ spectral index observed at the relative time $\sim 2\text{ hr}$ (Figure 5) may indicate a culmination of the He (re)acceleration, which, however, continues thereafter in a different regime. In event B the acceleration

persists for at least 10 hr. The culmination period corresponds to the position of the CME leading edge between 5–15 R_{\odot} (indicated with vertical dash-dot and dash-dot-dot lines in Figures 2, 4, and 5).

3.2. CME ASSOCIATION

Both SEP events were clearly associated with the constant-speed LASCO CMEs. The projected speed values were 880 km s^{-1} and 512 km s^{-1} for A and B, respectively. The CMEs seem fast enough to drive shocks. In the first event a signature of the shock is seen in the WIND/WAVES data (Figure 10). The shock speed near the Sun may be estimated using a frequency–height fit obtained with the Saito *et al.* (1970) density model for the fundamental emission. The resultant speed value is about 1200 km s^{-1} , and the extrapolated back-to-solar-surface start time is about 13:09 UT on 27 May 1998. This time falls close to the CME lift-off time estimated from the LASCO CME height–time data, $\approx 13:05 \text{ UT}$ (Figure 6). On the other hand, the speed $\approx 1200 \text{ km s}^{-1}$ seems consistent with a transit speed value, which might be estimated from the solar wind observations by the CELIAS Proton Monitor onboard SOHO (Hovestadt *et al.*, 1995), whereas the upstream solar wind speed was $\approx 350 \text{ km s}^{-1}$. For event B the solar wind data may indicate a transit speed of $\approx 620 \text{ km s}^{-1}$ and an upstream solar wind speed $\approx 450 \text{ km s}^{-1}$.

A CME lift-off should result in restructuring of corona magnetic fields behind it. Nitta and Akiyama (1999) proposed that occurrence of the flare-associated plasma ejections observed with *Yohkoh/SXT* depends on the presence of open magnetic field lines, which can be due to a preceding CME. Švestka *et al.* (1998) reported *Yohkoh/SXT* observations indicating that CMEs open the magnetic field, which thereafter stays partially open for at least tens of hours. Birn *et al.* (2000), using MHD simulations, investigated the dynamic evolution of three-dimensional magnetic field configurations, which may be relevant to the onset of a flare initiated after the eruption of a coronal mass ejection. They found topological changes, which could be the source of open flux tubes that are occasionally observed within CMEs. In some sets of simulations, they observed that a strongly localized electric field parallel to the magnetic field develops, which results in integrated voltages with maximum values of the order of a few hundred MeV, both on open and closed field lines. These results support an idea that a CME may trigger a flare behind it, and concurrently energetic particles might be produced and injected from behind the CME. In the case of the SEP events A and B, a number of changes in electromagnetic emissions were observed shortly before and after the first particle injection time, which may be considered as signatures of the restructuring processes initiated by the CME at different coronal altitudes well below the estimated altitude of the CME bow shock.

Kahler (1994) studied the *Skylab* and *Solwind* coronal mass ejections and found that nearly all $E > 10 \text{ MeV}$ solar energetic particle events are associated with fast ($> 400 \text{ km s}^{-1}$) CMEs. The peaks of injection profiles above 470 MeV occur when

CME heights reach 5–15 R_{\odot} or greater. In the five well-connected western events, the SEP injection was found to result from a single CME-driven shock, neither from the flare nor from coronal shocks. In Figures 2, 4, and 5, the vertical dot-dashed and dot-dot-dashed lines show the period when the CME is located between 5 R_{\odot} and 15 R_{\odot} from the solar center. First we note that the time profiles of both the proton and ${}^4\text{He}$ intensities, and of ${}^4\text{He}/p$ above 12.5 MeV nucl^{-1} are smooth when the distance of the CME is $> 15 R_{\odot}$. This might mean that after that distance the modification of spectral shapes of the proton and ${}^4\text{He}$ fluxes in interplanetary space is completed or greatly reduced. On the other hand, in the beginning, as mentioned, the rise profile is dominated by the injection process from the low solar atmosphere. However, one may expect that the transient processes and structures at different coronal altitudes beneath a CME, and the CME-driven interplanetary shock can affect the streaming flare particles. Recent observations of numerous shock waves at flanks and even at the rear end of some CMEs (Sheeley, Hakala, and Wang, 2000) give a reason to speculate that not only a single bow shock may be involved. Anyway continual streaming of accelerated ions during many hours after the flare, and also the dips and rebounds of intensities seen in the particle profiles of events A and B are signatures of the modification power of the CME.

3.3. COMPARISON WITH OTHER EVENTS

3.3.1. Typical ${}^3\text{He}$ -Rich Events

In the ${}^3\text{He}$ -rich events with ${}^3\text{He}/{}^4\text{He} \gtrsim 1$, the ${}^4\text{He}$ -to-proton flux ratio varies from 5% to about 40% (e.g., Figure 8 by Kocharov and Kocharov, 1984). Those events typically can be explained by an impulsive injection of flare accelerated particles. The duration of the events A and B is longer than is typical for the ${}^3\text{He}$ -rich events. In both events A and B, a significant ${}^3\text{He}$ flux enhancement in the energy range > 10 MeV nucl^{-1} was detected. However, the ${}^3\text{He}/{}^4\text{He}$ ratio was not very high, in the range 0.5–2.5%. The abundance of ${}^3\text{He}$ is still clearly above the standard solar ratio 0.05%. In the statistical survey of the Helios 1 and 2 observations (Hempe *et al.*, 1980; also Figure 5 by Kocharov and Kocharov, 1984) an event was listed with a ${}^3\text{He}/{}^4\text{He}$ ratio 1.2% and the maximum intensity of proton flux in the range 3.8–12.8 MeV nucl^{-1} about 150 $p/(\text{m}^2 \text{ s sr MeV})$, i.e., not far from the maximum proton intensity of A and B. Therefore, events A and B might be considered as a special type of ${}^3\text{He}$ rich events, probably as a kind of mixed (hybrid) events in the extended classification by Cliver (1996). Such events have attracted significantly less attention than the impulsive events with exceptionally high relative abundances of ${}^3\text{He}$, or the gradual events with the highest absolute fluxes of SEPs.

3.3.2. Large SEP Events during 1990–1991

The ${}^3\text{He}/{}^4\text{He}$ ratios for SEPs over the high-energy range 50–110 MeV nucl^{-1} were determined by Chen, Guzik, and Wefel (1995) using helium data measurements of the ONR-604 instrument onboard the *CRRES* mission. For the 1990–1991

solar maximum period they identified thirteen events with ${}^3\text{He}/{}^4\text{He}$ ratio larger than 0.5%. In particular during 23–24 March 1991 the ${}^3\text{He}/{}^4\text{He}$ ratio rose above 15% (also Clayton, Guzik, and Wefel, 2000). This event was associated with impulsive solar flare on 22 March 1991 (X9.4/3B), chromospheric Moreton wave (speed $\approx 1900 \text{ km s}^{-1}$), and coronal and interplanetary shocks with speeds $\approx 1400\text{--}1500 \text{ km s}^{-1}$ (Ermakov *et al.*, 1993; Kocharov *et al.*, 1995). Clayton, Guzik, and Wefel (2000) pointed out that the 23–24 March ${}^3\text{He}/{}^4\text{He}$ -enhancement occurs in coincidence with the helium intensity peak, which is consistent with an enrichment of ${}^3\text{He}$ near the interplanetary shock. However, a question as to what is the initial progenitor of the interplanetary-shock-accelerated ${}^3\text{He}$ -rich particle population has not been raised in those papers.

In the case of the 11 June and 15 June 1991 events, Chen, Guzik, and Wefel (1995) noted a correlation between the inferred proton/helium spectral index from the γ -ray measurements and the corresponding SEP spectral indices, suggesting that the high-energy SEPs may come from the same acceleration event as the particles that interact at the Sun and produce γ -rays. However, Kocharov *et al.* (1994a) found that the interacting particle spectrum in the 15 June 1991 event was slightly softer than the interplanetary particle (SEP) spectrum, whereas the total number of $\gtrsim 10 \text{ MeV}$ protons was comparable. That let those authors propose that the interplanetary protons originate from the same population of accelerated particles as the interacting ones, and some re-acceleration process operating higher in the solar corona is responsible for the hardening of the proton spectrum before their injection into the interplanetary medium.

Extensive studies of the 24 May 1990 solar flare and SEP event revealed that in the 100–1000 MeV range the energy spectrum of protons interacting at the Sun late in the γ -ray/neutron flare was similar but slightly softer than the spectrum of the first-period (prompt) protons injected into the interplanetary medium, whereas the interacting-to-interplanetary proton ratio was of order of unity (Kocharov *et al.*, 1994b, 1996; Torsti *et al.*, 1996). At the same time, a delay of about 10 min in the injection of first SEPs rules out a direct escape of flare particles into the interplanetary medium. These facts taken together might be interpreted in terms of short-period trapping and coronal re-acceleration of the flare particle population. Note that in the case of the 24 May 1990 event a second (delayed) period of SEP production was also identified, which is the continual acceleration at the CME-driven shock in the interplanetary medium.

3.3.3. CME Associated Events during 1996–1999

Careful studies of the 9 July 1996 SEP event observed by ERNE/SOHO (Laitinen *et al.*, 2000, and references therein) revealed two periods of SEP production in that event associated with an impulsive flare (S10 W30) and CME. The maximum of the first period injection of SEPs was observed 50 min after the flare pulse. Shocks and other transient processes in the solar corona associated with reconfiguration of coronal magnetic fields during the CME lift-off were regarded as a possible source

of this component. The second period of SEP injection continued for many hours, and the interplanetary shock acceleration provides a straightforward explanation for this component of SEPs. The two components differ in the energy spectrum, but no difference in the He/p ratio is found. Observed abundances, ${}^4\text{He}/\text{p} = 0.12 \pm 0.02$ and ${}^3\text{He}/{}^4\text{He} \approx 0.02$, might be explained by re-acceleration of flare particles.

The 9 July 1996 event occurred under the very quiet interplanetary transport conditions, the parallel mean free path was in excess of 1 AU, so that ‘seeing’ of the SEP source was exceptionally good, and precise injection profiles have been deduced. In contrast, the 27 May 1998 and 28 December 1999 periods were not so transparent in terms of the SEP transport. This significantly limits the capability to deduce the injection profiles of SEPs. Available proton anisotropy data and intensity-time profiles definitely indicate that SEP injection continued for many hours after the flares, so that interplanetary shock acceleration should be involved. The fine time structure of the near-Sun production could not be resolved, but it cannot be ruled out that the scenario of the first-hour injection was similar to that deduced for the 9 July 1996 event. The first SEP production should be followed by at least a several-hours-long re-acceleration at the CME-driven shock in the interplanetary medium.

Statistical studies of the SEP-CME-flare relations can also contribute to understanding of the energetic particle sources. In particular, Torsti *et al.* (1998) studied SEP events associated with large Earth-directed CMEs observed during January–May 1997. Based on analysis of the SEP-event-associated electromagnetic emissions, it was concluded that the potential of CMEs to produce accelerated particles in the interplanetary medium crucially depends on the solar eruption evolution below $\approx 2 R_{\odot}$, and all available data are in agreement with the hypothesis that a seed population for the interplanetary CME-driven shock acceleration is produced in the solar corona during an early phase of the eruption. The seed-population hypothesis found indirect support in the recent statistical study by Kocharov *et al.* (2001). Those authors also argued in favor of the scenario that an early rise of CME triggers the flare which in its turn starts a proton acceleration continuing later at the CME-driven shock in the interplanetary medium. One can see that such a ‘closed-chain scenario’ fits well what we observe in the 27 May 1998 and 28 December 1999 events (e.g., Figure 6).

3.3.4. Large SEP Events with ${}^3\text{He}$ Enhancement during 1997–2000

Mason, Mazur, and Dwyer (1999) reported the ${}^3\text{He}$ abundance at ≈ 0.5 – 2 MeV nucl^{-1} energies in 12 large, interplanetary shock associated SEP events. In five of the events, the ${}^3\text{He}$ intensity-time profile was similar to the ${}^4\text{He}$ intensity-time profile, indicating a common acceleration and transport origin for the two species. The average ${}^3\text{He}/{}^4\text{He}$ ratio was about 0.2%, a factor ≈ 5 over the solar wind value. The recent search by Desai *et al.* (2001) has revealed 25 similar events with the enhancement factors from ~ 3 to 600 over the solar wind value. The authors suggested that ${}^3\text{He}$ enhancements at interplanetary shocks reflect the availability

of seed particles that originated previously in impulsive flares. It was also found that the low-energy ^3He and Fe remnants from impulsive events are present in a majority of quieter periods. Mason, Mazur, and Dwyer (1999) suggested that these suprathermal ions may therefore be a source population that is available for further acceleration by interplanetary shocks that accompany large SEP events, thereby leading to the ^3He enhancements in a significant fraction of large SEP events.

We reason that if the seed population of flare particles may be present even at 1 AU, it should especially exist near the Sun, being strongly enhanced in the corresponding range of solar longitudes shortly after the flare. Such a hypothesis could explain what we observe in the 27 May 1998 and 28 December 1999 events. It is also possible that different seed populations may dominate in different eruptions, or in the same eruption but observed at very different solar longitudes.

Acknowledgements

The authors wish to thank Henry Aurass for supplying the Trenseldorf radio spectra. The Nançay radioheliograph quick-look images are prepared by the radio group at DASOP, Observatoire de Paris, and they can be obtained via the BASS2000 Web archive. The Hiraïso radio spectrograph data are supplied by the Communications Research Laboratory, Japan, and available at their Webpage. *Yohkoh* is a Japanese solar mission, with several internationally operated instruments. The *Yohkoh* data archive at ISAS, Sagamihara, was used for this study. The Compton Gamma Ray Observatory BATSE solar data are made available by the Solar Data Analysis Center (SDAC) at Goddard Space Flight Center, through their Web data archive. The SWEPAM/*ACE* data are archived at California Institute of Technology. We thank the CELIAS team for the solar wind data available in the SOHO archive. The ERNE team is financially supported by the Academy of Finland. SOHO is an international cooperation project between ESA and NASA.

References

- Birn, J., Gosling, J. T., Hesse, M., Forbes, T. G., and Priest, E. R.: 2000, *Astrophys. J.* **541**, 1078.
 Bochsler, P.: 1998, *Space Sci. Rev.* **85**, 291.
 Breneman, H. H. and Stone, S. C.: 1985, *Astrophys. J.* **299**, L57.
 Brueckner, G. E., Howard, R. A., Koomen, M. J., Korendyke, C. M., Michels, D. J., Moses, J. D., Socker, D. G., Dere, K. P., Lamy, P. L., Llebaria, A., Bout, M. V., Schwenn, R., Simnett, G. M., Bedford, D. K., and Eyles, C. J.: 1995, *Solar Phys.* **162**, 357.
 Cane, H., Reames, D. V., and von Rosenvinge, T. T.: 1991, *Astrophys. J.* **373**, 675.
 Chen, J., Guzik, T. G., and Wefel, J. P.: 1995, *Astrophys. J.* **442**, 875.
 Clayton, E. G., Guzik, T. G., and Wefel, J. P.: 2000, *Solar Phys.* **195**, 175.
 Cliver, E. W.: 1996, in R. Ramaty, N. Mandzhavidze, and X.-M. Hua (eds.), *High Energy Solar Physics, AIP Conf. Proc.* **374**, 45.

- Delaboudinière, J.-P., Artzner, G. E., Brunaud, J., Gabriel, A. H., Hochedez, J. F., Millier, F., Song, X. Y., Au, B., Dere, K. P., Howard, R. A., Kreplin, R., Michels, D. J., Moses, J. D., Defise, J. M., Jamar, C., Rochus, P., Chauvineau, J. P., Marioge, J. P., Catura, R. C., Lemen, J. R., Shing, L., Stern, R. A., Gurman, J. B., Neupert, W. M., Maucherat, A., Clette, F., Cugnon, P., and van Dessel, E. L.: 1995, *Solar Phys.* **162**, 291.
- Desai, M. I., Mason, G. M., Dwyer, J. R., Mazur, J. E., Smith, C. W., and Skoug, R. M.: 2001, *Astrophys. J.* **553**, L89.
- Ermakov, S. I., Kontor, N. N., Lyubimov, G. P., Pavlov, N. N., Tulupov, V. I., Chuchkov, E. A., and Shcherbovskij, B. Ya.: 1993, *Izvestija Ross. Akad. Nauk, Ser. Fiz.* **51**, 7.
- Feldman, U.: 1998, *Space Sci. Rev.* **85**, 227.
- Geiss, J.: 1998, *Space Sci. Rev.* **85**, 241.
- Gloeckler, G. and Geiss, J.: 1989, in C. J. Waddington (ed.), *Cosmic Abundances of Matter*, AIP Conf. Proc. **183**, 49.
- Hansteen, V. H., Leer, E., and Holzer, T. E.: 1997, *Astrophys. J.* **482**, 498.
- Hempe, H., Müller-Mellin, R., Kunow, H., and Wibberenz, G.: 1980, *Proc. 16th Int. Cosmic Ray Conf., Kyoto* **5**, 95.
- Hovestadt, D., Hilchenbach, M., Bürgi, A., Klecker, B., Laeverenz, P., Scholer, M., Grünwaldt, H., Axford, W. I., Livi, S., Marsch, E., Wilken, B., Winterhoff, H. P., Ipavich, F. M., Bedini, P., Coplan, M. A., Galvin, A. B., Gloeckler, G., Bochsler, P., Balsinger, H., Fisher, J., Geiss, J., Kallenbach, R., Wurz, P., Reiche, K.-U., Gliem, F., Judge, D. L., Ogawa, H. S., Hsieh, K. C., Möbius, E., Lee, M. A., Managadze, G. G., Verigin, M. I., and Neugebauer, M.: 1995, *Solar Phys.* **162**, 441.
- Kahler, S.: 1994, *Astrophys. J.* **428**, 837.
- Kerdran, A. and Delouis, J.: 1997, in G. Trottet (ed.), *Coronal Physics from Radio and Space Observations*, Proc. CESRA Workshop, Springer-Verlag, Berlin, p. 192.
- Klein, K.-L., Khan, J. I., Vilmer, N., Delouis, J.-M., and Aurass H.: 1999, *Astron. Astrophys.* **346**, L53.
- Kocharov, L. G. and Kocharov, G. E.: 1984, *Space Sci. Rev.* **38**, 89.
- Kocharov, G. E., Kovaltsov, G. A., and Kocharov, L. G.: 1983, *Proc. 18th Int. Cosmic Ray Conf., Bangalore* **4**, 105.
- Kocharov, L. G., Kovaltsov, G. A., Kocharov, G. E., Chuikin, E. I., Usoskin, I. G., Shea, M. A., Smart, D. F., Melnikov, V. F., Podstrigach, T. S., Armstrong, T. P., and Zirin, H.: 1994a, *Solar Phys.* **150**, 267.
- Kocharov, L. G., Lee, J. W., Zirin, H., Kovaltsov, G. A., Usoskin, I. G., Pyle, K. R., Shea, M. A., and Smart, D. F.: 1994b, *Solar Phys.* **155**, 149.
- Kocharov, L. G., Lee, J. W., Wang, H., Zirin, H., Kovaltsov, G. A., and Usoskin, I. G.: 1995, *Solar Phys.* **158**, 95.
- Kocharov, L. G., Torsti, J., Vainio, R., Kovaltsov, G. A., and Usoskin, I. G.: 1996, *Solar Phys.* **169**, 181.
- Kocharov, L., Vainio, R., Torsti, J., and Kovaltsov, G. A.: 1998, *Solar Phys.* **182**, 195.
- Kocharov, L., Torsti, J., St. Cyr, O. C., and Huhtanen, T.: 2001, *Astron. Astrophys.* **310**, 1064.
- Kozlovsky, B. and Ramaty, R.: 1974, *Astrophys. J.* **191**, L43.
- Laitinen, T., Klein, K.-L., Kocharov, L., Torsti, J., Trottet, G., Bothmer, V., Kaiser, M. L., Rank, G., and Reiner, M. J.: 2000, *Astron. Astrophys.* **360**, 729.
- Laming, J. M. and Feldman, U.: 1994, *Astrophys. J.* **426**, 414.
- Laming, J. M. and Feldman, U.: 2001, *Astrophys. J.* **546**, 552.
- Mandzhavidze, N., Ramaty, R., and Kozlovsky, B.: 1997, *Astrophys. J.* **489**, L99.
- Mandzhavidze, N., Ramaty, R., and Kozlovsky, B.: 1999, *Astrophys. J.* **518**, 918.
- Mann, G., Aurass, H., Voigt, W., and Paschke, J.: 1992, *Proc. 1st SOHO Workshop*, ESA SP-348, 129.
- Mason, G. M., Mazur, J. E., and Dwyer, J. R.: 1999, *Astrophys. J.* **525**, L133.

- McComas, D. J., Bame, S. J., Barker, P., Feldman, W. C., Phillips, J. L., Riley, P., and Griffée, J. W.: 1998, *Space Sci. Rev.* **86**, 563.
- Meyer, J.-P.: 1985, *Astrophys. J. Suppl.* **57**, 151.
- Murphy, R. J., Share, G. H., Grove, J. E., Johnson, W. N., Kinzer, R. L., Kurfess, J. D., Strickman, M. S., and Jung, G. V.: 1997, *Astrophys. J.* **490**, 883.
- Neugebauer, M.: 1981, *Fund. Cosmic Phys.* **7**, 131.
- Ng, C. K., Reames, D. V., and Tylka, A. J.: 1999, *Geophys. Res. Lett.* **26**, 2145.
- Nitta, N. and Akiyama, S.: 1999, *Astrophys. J.* **525**, L57.
- Ramaty, R., Colgate, S. A., Dulk, G. A., Hoyng, P., Knight, J. W., III, Lin, R. P., Melrose, D. B., Paizis, C., Orrall, F., and Shapiro, P. R.: 1978, *Proc. 2nd Skylab Workshop on Solar Flares*, Chapter 4, NASA Boulder, Colorado.
- Reames, D. V.: 1994, *Adv. Space Res.* **14**, 177.
- Reames, D. V.: 1999, *Space Sci. Rev.* **90**, 413.
- Reames, D. V., Cane, H. V., and von Rosenvinge, T. T.: 1990, *Astrophys. J.* **357**, 259.
- Reames, D. V., Ng, C. K., and Tylka, A. J.: 2000, *Astrophys. J.* **531**, L83.
- Reames, D. V., Richardson, I. G., and Barbier, L. M.: 1991, *Astrophys. J.* **382**, L43.
- Saito, K., Makita, M., Nishi, K., and Hata, S.: 1970, *Ann. Tokyo Astron. Obs.* **12**, 51.
- Schwartz, R. A., Fishman, G., Meegan, C., Wilson, R., and Paciesas, W.: 1993, *Adv. Space Res.* **13**, 233.
- S.G.D.: 1998, *Solar Geophysical Data, NOAA Prompt and Comprehensive Reports* **647** part I, **651** part II.
- S.G.D.: 2000, *Solar Geophysical Data, NOAA Prompt Reports* **665** part I, **666** part I.
- Share, G. H. and Murphy, R. J.: 1997, *Astrophys. J.* **485**, 409.
- Share, G. H. and Murphy, R. J.: 1998, *Astrophys. J.* **508**, 876.
- Sheeley Jr., N. R., Hakala, W. N., and Wang, Y.-M.: 2000, *J. Geophys. Res.* **105**, 5081.
- Švestka, Z., Fárnik, F., Hudson, H. S., and Hick, P.: 1998, *Solar Phys.* **182**, 179.
- Torsti, J., Valtonen, E., Lumme, M., Peltonen, P., Eronen, T., Louhola, M., Riihonen, E., Schultz, G., Teittinen, M., Ahola, K., Holmlund, C., Kelhä, V., Leppälä, K., Ruuska, P., and Strömmer, E.: 1995, *Solar Phys.* **162**, 505.
- Torsti, J., Kocharov, L. G., Vainio, R., Anttila, A., and Kovaltsov, G. A.: 1996, *Solar Phys.* **166**, 135.
- Torsti, J., Anttila, A., Kocharov, Mäkelä, P., Riihonen, E., Sahla, T., Teittinen, M., Valtonen, E., Laitinen, T., Vainio, R.: 1998, *Geophys. Res. Lett.* **25**, 2525.
- Tsuneta, S., Acton, L., Bruner, M., Lemen, J., Brown, W., Carvalho, R., Catura, R., Freeland, S., Jurcevich, B., and Owens, J., 1991, *Solar Phys.* **136**, 37.
- Van Hollebeke, M. A. I.: 1975, *Proc. 14th Int. Cosmic Ray Conf., München* **5**, 1563.